

EXPERIMENTAL INVESTIGATION ON THE EFFECT OF EQUIPMENT STRUCTURE ON REFRIGERATION PERFORMANCE OF COMBINED MAGNETIC REFRIGERATION SYSTEM

Lijuan He^{1,}, Ningyu Sun¹, Yuze Han², Wenxuan Yang¹, Jiaohong Huang³*

¹ Inner Mongolia University of Science and Technology, Baotou 014010, China

² Guilin University of Technology, Guilin 541000, China

³ Baotou Research Institute of Rare Earths, Baotou 014030, China

* Corresponding author; E-mail address: zdlilyhe@163.com

A combined magnetic refrigeration system that consists of external rotating magnetic field part of the rotary magnetic refrigerator and the flow path of the reciprocating magnetic refrigeration part was presented in this work. Experiments were carried out to investigate the influence of the structure for heat exchanger and active regenerator port on the refrigeration performance. With an operating frequency of 0.2 Hz and a magnetic field varying from 0 to 1.3 T, a 22.2 K temperature span has been obtained when the heat exchanger with inner threaded coil tube was applied in the cold end. On the research of the hot end structure, the refrigeration temperature span of the plate heat exchanger is 22.7 K, the temperature of the cold end with fans is 6 K lower than that of the heat exchanger without fans. A 24.1 K temperature span of the combined magnetic refrigeration system can be obtained when the gradually varied port is used to the active magnetic regenerator.

Key words: combined magnetic refrigeration system, equipment structure, heat exchangers, temperature span, rare earth materials

1. Introduction

With the development of refrigeration technology, the traditional refrigeration technology such as compression and ejection refrigeration technology [1, 2], the refrigerant used will cause some serious environmental problems. Magnetic refrigeration technology is a new type of environment-safe and reliable operation refrigeration technology. In the magnetic refrigeration system, a magnetocaloric material (MCM) with magnetocaloric effect (MCE) is used as a refrigerant. It has high research value and great applicable prospects. Many efforts [3-11] have been made to study the temperature span and refrigeration performance of magnetic refrigeration systems based on experimental analysis. In order to optimize the performance of the magnetic refrigeration system, a permanent-magnet rotary refrigerator with spherical granular working materials was presented by Zimm, C. *et al.* [12]. The system performance of working materials Gd, GdEr and LsFeSiH were tested respectively, while the operating frequency of the system was 0.5-4.0 Hz. A temperature span of 25 K can be obtained when the working materials gadolinium (Gd) and gadolinium erbium ball particles (Gd-Er) are filled at that time. Engelbrecht, K. *et al.* [13] designed and tested a rotary active magnetic regenerator device. The maximum temperature span was 25.4 K in the no-load state, with an operating frequency of 2 Hz.

Lupponglung, V. *et al.* [14] designed and assembled a rotary magnetic refrigeration prototype that used rotating magnet to provide a magnetic field of 0 - 0.65 T. The flow rate was limited to 0.5 L/min, which resulted in insufficient heat transfer rate by the slow heat exchange fluid flow, and the maximum temperature span was measured to be 0.5 K. Huang, B. *et al.* [15] presented a rotary active magnetic regeneration refrigerator prototype, which was developed for studying the performance of different magnetocaloric materials in a realistic practical environment. Gadolinium was used as the MCM, on the condition of an AMR frequency of 1.7 Hz, a flow rate of 4.34 l min⁻¹ and a hot end temperature of 295 K, the maximum zero power temperature span is 11.6 K. The connection of circulation path in magnetic refrigeration system is also worth studying. Consisting of permanent magnet, AMR bed, pumps, hydraulic circuit, active magnetic double regenerator cycle (AM2RC) and control subsystem, the detailed design of a room-temperature magnetic refrigerator has been presented by Zheng, H. Y., *et al.* [16] in 2009. Based on the finite element method (FEM) of numerical simulation, the magnetic flux sources have been optimized by a geometrical change of magnetic structure. By using the optimized structure, the weight of permanent magnet NdFeB can be reduced by about 40%. After employing two hydraulic circuits, the performance of magnetic refrigeration has been improved.

A detailed performance analysis needs to be done for active magnetic regenerator, one of the key equipment of magnetic refrigeration system. Arnold, D.S. *et al.* [17] determined the performance of a two-material, layered AMR in terms of temperature span, cooling power, and efficiency. Results suggest that the largest temperature spans are expected to occur when each material is operating with its average temperature near their Curie temperatures. Balli, M. *et al.* [18] designed and built a linear reciprocating permanent magnet cooling system. In order to reduce the energy consumption and increase the thermodynamic performances of the magnetic system, a special configuration of the magnetocaloric materials is developed. The numerical results about the applied magnetic forces on the configuration were analyzed. The machine was designed to produce cooling power between 80 and 100 W with a temperature span larger than 20 K. Romero Gómez, J. *et al.* [19] produced a reciprocating regenerator magnetic refrigeration system. Distilled water as the heat transfer fluid (HTF) with a mass of 180g Gd is used for this system. A 3.5 K temperature span can be obtained when the magnetic field was 1 T. A reversing valve to change the flow direction was used, which effectively reduced the dead volume effect of the heat transfer fluid. Velázquez, C. *et al.* [20] designed, built and tested a new versatile room temperature reciprocating magnetic refrigeration demonstrator. A Halbach Nd₂e₁₄B permanent magnet with a slot of 10 mm width has been used to generate the magnetic field with a maximum value of 1.4 T. The new demonstrator achieved a maximum no-load temperature span of 19.3 K at a certain range of operating frequencies. The advantages and disadvantages of reciprocating and rotary magnetic refrigerators were compared and summarized by Romero Gómez, J. *et al.* [21]. Results showed that the performance of the reciprocating system was relatively reliable, but the operating frequency and mechanical efficiency were limited by the excessive equipment volume and inertia force. Rotating equipment was less affected by inertial force, which was different from reciprocating system. Totally, there were more complex sealing and leakage problems, which could be found of rotating machinery in practical applications.

However, the reciprocating room temperature magnetic refrigerator cannot achieve a higher cooling effect because of the limitation of its cycle frequency by the principle. Although the rotary room temperature magnetic refrigerator can reach a high frequency, its heat exchange system is

complex and the failure rate is high. In order to avoid these shortcomings, a new type of combined magnetic refrigeration system (CMRS) was proposed in this paper. The effect of several structural parameters on the performance of CMRS was investigated.

2. Experimental Rig

2.1. Description of the combined magnetic refrigeration system

CMRS consists of two parts, which are the external rotating magnetic field part of the rotary magnetic refrigerator and the flow path of the reciprocating magnetic refrigeration part. The structure of CMRS is made up of external magnetic field system, active magnetic regenerator (AMR), cold end heat exchanger, hot end heat exchanger and cold chamber, five parts. Figure 1 is the physical picture of combined magnetic refrigeration machine.



Fig. 1. CMRS

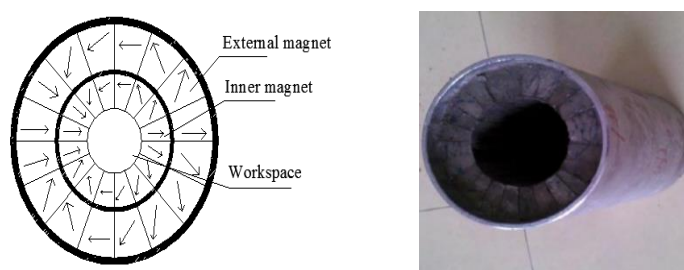


Fig. 2. Structure diagram of double layer nested permanent magnet group

The permanent magnet group system of the CMRS is composed of two sets of double layer nested circular cylindrical concentric Halbach permanent magnets. The structure of each set of double-layer nested permanent magnet group is shown in Fig. 2. Each set of permanent magnet group includes 16 Halbach permanent magnet blocks inside and outside its cylinder. When the internal magnetic field rotates by generating periodic magnetic field, it will produce magnetic thermal effect. During the working space, the AMR is placed at the center of the magnetic field, which is synchronized through the gears. The AMR shown in Fig. 3 involves regenerator shell, regenerator ports (cold and hot ends) and regenerator filler (magnetic materials (Figs. 4 and 5)). The regenerator shell adopts random co-polypropylene tube (PPR tube), with the length and wall thickness of 290 mm and 3.3 mm, respectively. In this research, two different types of ports structures are applied to compare the effect of system performance, which are gradually varied port and suddenly varied port. The number of filled layers of the magnetic working substance Gd spherical particles is single layer, and the Curie temperature is 293.15 K. The filling length set in the experiment accounts for 100% of the total length of active magnetic regenerator (AMR). Other relevant parameters of Gd sphere particles are listed in Tab. 1.



Fig. 3. AMR

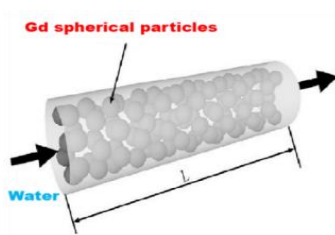


Fig. 4. Schematic diagram of AMR filling



Fig. 5. Gd spherical particles

Table 1. Experimental parameters

| Label | Equipment |
|----------------------------------|-----------------|
| Magnetocaloric material | Gadolinium (Gd) |
| Packing quality (g) | 1680 |
| Packing size (mm) | 0.6-0.85 |
| Packing length (mm) | 250 |
| Regenerator diameter (mm) | 30 |
| Magnetic field (T) | 0-1.3 |
| Room temperature (K) | 293 |
| Heat exchange zone angle (°) | 20 |
| Non-heat exchange zone angle (°) | 160 |
| Operating frequency (Hz) | 0.2 |

2.2. Experimental principle of the combined magnetic refrigeration system

The structural principle of CMRS is shown in Fig. 6. The device names corresponding to the numbers shown in Fig. 6 are listed in Tab. 2. To achieve continuous refrigeration cycle, there are four adjustment processes to valve system in magnetic refrigeration system. The existence of phase difference between permanent magnet groups causes a process of magnetize and demagnetize to 1-1 permanent magnet group 1 and 1-2 permanent magnet group 2, respectively. Then the 2-1 magnetic materials' temperature increases while the 2-2 magnetic materials' temperature decreases. On the first stage, the valve system is adjusted that make the heat transfer fluid (HTF) pass through the hot end heat exchanger (HEX 7) only, with no HTF in two groups of AMR. Considering the influence of corrosion, and weakly alkaline deionized water (PH=12), is selected as heat transfer fluid (HTF). On the stage of the second adjustment of the valve system, the HTF flows in the direction of the thin arrow driven by the water pump. The HTF of the cold end HEX 6 absorbs the magnetic materials' heat when it passes through the AMR 2-1, meanwhile, releases heat at hot end HEX 7. Then the residual heat of HTF is absorbed by the other magnetic materials when it passes through the AMR 2-2. The HTF temperature decreases, which could refrigerate the cold end HEX 6. Thirdly, some further adjustments have been made to the valve system, where the HTF only passes through hot end HEX 7. The magnetic fields of 1-1 and 1-2 are deflected, which cause 1-1 to be in a demagnetized process and 1-2 in an excited progress. The AMR 2-1 magnetic materials temperature decreases, on the contrary, the AMR 2-2 magnetic materials temperature increases. Next, the HTF flows in the direction of the thick arrow driven by the water pump. The valve system is finally adjusted and the HTF flows according to the direction of the thick arrow.

The HTF of the cold end HEX 6 absorbs the magnetic material's heat when it passes through the AMR 2-2, releasing heat at hot end HEX 7 at the same time. Then the after heat of HTF is absorbed by other magnetic materials when HTF passes through the AMR 2-1. The HTF temperature decreases, resulting in the refrigeration of the cold end HEX 6. So far, a refrigeration cycle has been completed after four times of the valve system adjustments. The operating parameters of the experiment are listed in Tab. 1. Heat transfer zone refers to the process in which heat transfer fluid passes through magnetic materials and generates heat exchange with magnetic materials. The non-heat transfer zone indicates that the magnetic working medium is undergoing adiabatic magnetization or adiabatic demagnetization process, and the HTF does not pass through the magnetic working medium in this

process. Different heat exchange angles have an impact on refrigeration performance. Schematic diagram of heat transfer zone and non-heat transfer zone of magnetic field are shown in Fig. 7. In the experiment, the angle of the heat exchange zone was set to 20° .

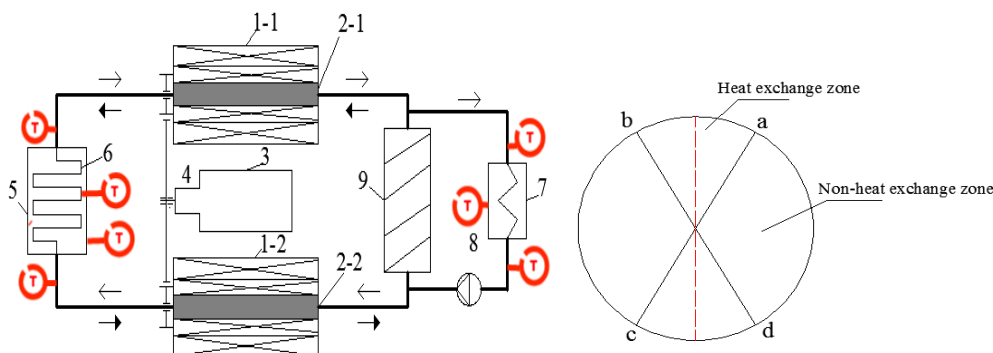


Fig. 6. Schematic diagram of the CMRS Fig. 7. Heat transfer zone and non-heat transfer zone

Table 2. Equipment label of CMRS

| Label | Equipment |
|-------|-------------------------------------|
| 1-1 | concentric permanent magnet group 1 |
| 1-2 | concentric permanent magnet group 2 |
| 2-1 | active magnetic regenerator 1 |
| 2-2 | active magnetic regenerator 2 |
| 3 | servo motor |
| 4 | planetary reducer |
| 5 | cold chamber |
| 6 | cold end heat exchanger |
| 7 | hot end heat exchanger |
| 8 | water pump |
| 9 | valve system |

2.3. Data acquisition system

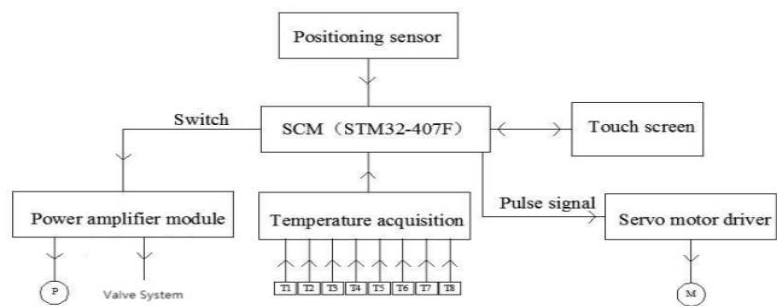
The data acquisition system is applied to collect temperature, velocity and flow information, which are composed of temperature sensor, electromagnetic flow-meter, Gauss meter, hot-bulb anemometer, cryogenic thermostat and a variable temperature measuring instrument. Eight PT100 temperature sensors are set in certain areas, which include two hot end ports, two cold end ports, laboratory environment, outer surface of the hot end HEX and cold end HEX, and cold chamber space. The location of the specific temperature sensor has been marked with a red "T" in Fig. 6. Other measuring instrument parameters are listed in Tab. 3.

2.4. Control system

The combined magnetic refrigerator control system is shown in Fig. 8. The main control is performed by a single-chip microcomputer (STM32-407F). The single-chip microcomputer controls the power amplifier module and the servo driver respectively by outputting the switch value and pulse signal. The power amplifier module controls the diaphragm pump and solenoid valves by outputting signals.

Table 3. Measuring instrument parameters

| Instrument | model | range | accuracy |
|----------------------------|---------------|----------|-------------|
| Temperature sensor (K) | PT100 | 233-673 | $\pm 0.15K$ |
| Electromagnetic flowmeters | JSWS-WWWY-LFA | 0.16-2.5 | 0.5% |
| Gauss meter (mT) | HT201 | 0-200mT | $\pm 2\%$ |
| Hot bulb anemometer (m/s) | QDF-3 | 0.05-30 | $\pm 4\%$ |
| cryogenic thermostat (K) | DC-2060 | 253-373 | 0.01K |

**Fig. 8. Magnetic refrigerator control structure diagram**

3. Results and discussion

Heat exchangers (cold end exchanger and hot end exchanger), and active regenerator ports, are key equipment in the refrigeration system. Based on the combined magnetic refrigeration system, the performance of the structure parameters for key equipment are assessed.

3.1. Effect of cold end structure on the system performance

3.1.1 Effect of tube length of heat exchanger

The temperature values for three heat transfer areas are compared in Fig. 9. The temperature at the hot end decreased as the tube length increasing. It is because that the increase of tube length caused the increase of circulating water in the system, and the heat released by the magnetothermal effect was finite. The temperature change of HTF would decrease with the increase of circulating water quantity. Owing to the finite of the magnetic material's refrigeration capacity, with the systems' circulating water increasing, the temperature change produced slightly. And this led to an increase in the cold end temperature (T_c) when the heat exchangers' tube length increased. The cold chamber's temperature (T_{cc}) shows a downward trend and later flattens. Attributing to the increase of heat transfers' area caused by increased length, the heat exchange capacity between the heat exchanger and the cold chamber was enhanced. However, due to the limited cooling capacity of the magnetic material, the length of the heat exchanger cannot be excessively increased, and the temperature of the cold chamber of the system would not continue to decrease. In later investigations, the inner diameter and length of the cold-end heat exchanger coils will remain 6mm and 12mm, respectively.

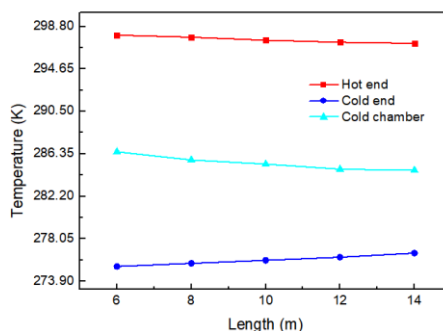


Fig. 9. Temperature distribution vs the tube length

3.1.2 Effect of cold end HEX structure on the system performance

In this experiment, structures of the inner threaded coil tube and the structure of outer finned coil tube are applied. When the magnetic refrigeration system works, the HTF absorbing heat generated by excitation releases heat at the hot end of the system, and the low temperature HTF reaches the cold end for refrigeration. As time goes by, the value of T_h increases, and the T_c decreases. Figure 10 respectively illustrates temperature variation versus time for both inner threaded coil tubes and outer finned coil tubes.

As can be seen from Fig. 10 (a), all the curves show the same trends. Under the same working conditions, the temperature of the heat exchanger (T_{HEX}) with inner surface threaded coils is 0.9 K, which is higher than that with smooth inner surface coils. Besides, the T_{HEX} with the inner threaded coil tube is 0.6 K lower than that with outer fins.

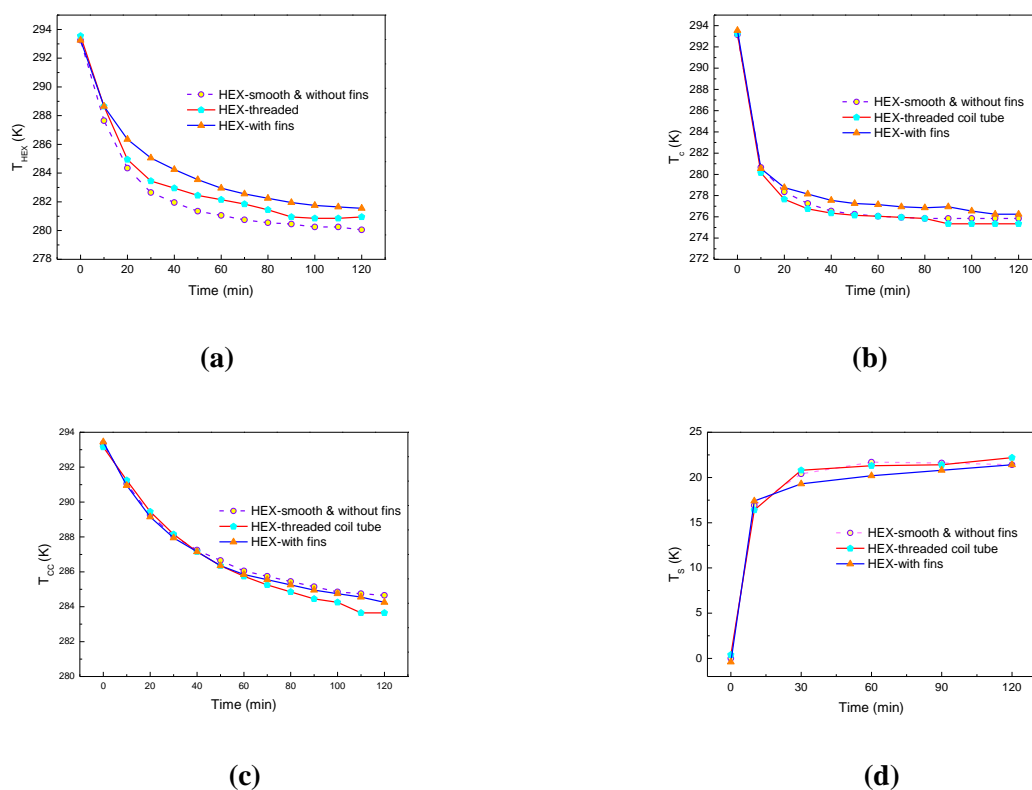


Fig. 10. Effect of inner and outer surface structures of heat exchange

As shown in Fig. 10 (b), the T_c with inner surface threaded coils is lower than with smooth coils. That is to say, threaded coil tubes have strengthened the heat exchange ability. The T_c with inner threaded coil tube is about 1 K lower than that of outer coil with fins. As shown in Fig. 10 (c), The T_{cc} with surface threaded coil is 1 K lower than the inner surface smooth coil. This is because that the heat transfer convection capacity of coil tube increases when the HTF flows on the threaded inner surface, which leads to the T_{cc} decreases and reaches the purpose of heat exchange. The T_{cc} with fins is half a K lower than without fins. The evaluation index of magnetic refrigeration system performance is the temperature span.

Figure 10 (d) presents the variation of temperature span (T_s) for three models. The T_s obtained with finned HEX or HEX with smooth coil tube both are 21.4 K, which are 0.8 K lower than that with inner threaded coil tube. Based on the result of the above analysis, it can be concluded that HEX with inner-surface threaded coils tube and outer-surface fins could also decrease the T_{cc} . The performance of the inner threaded coil tube can be better than that of the outer finned coil tube.

3.2. Effect of hot end structure type on the system performance

3.2.1 Effect of heat exchanger structure type

Figure 11 shows the effect of hot end HEX type of system performance. Two G12308HA2SL fans (Guangdong, China, 201 m³/h) are applied to the system. It is shown in Fig. 11 (a) that the T_c using plate HEX is 1.1 K lower than the tube HEX, and the T_h using plate HEX is 0.8 K lower than the tube HEX. This is because the heat transfer coefficient of the plate HEX is larger than tube HEX, and the heat released from the hot end can be dissipated in time. As a result, the bigger the temperature span, the better the performance will be.

As shown in Fig. 11 (b), the plate HEX has a refrigeration temperature of 22.7 K, which is 2.5 K higher than the tube HEX. This is further indicated that the refrigeration performance of the plate HEX is superior to the tube HEX. The data from the experiment shows that the plate HEX is more suitable for the combined magnetic refrigeration system. Tura, A. *et al.* [22] adopted the aluminum plate heat exchanger and used metal gadolinium and gadolinium alloy as magnetic working medium, and obtained a temperature span of about 22.5 K when the hot end temperature was 298 K. Under the same hot end temperature, the temperature span of 22.7 K obtained by the combined magnetic refrigeration system (CMRS) is relatively close.

3.2.2 Effect of heat dissipation mode of heat exchanger

Figure 12 shows the variations of the temperature for natural convection and forced convection condition with time going by. As can be seen, the T_h with fans is 8 K lower than the HEX without fans, and the T_c with fans is 6 K lower than the heat exchanger without fans. The decrease in the T_c is due to the heat of the heat exchanger being dissipated quickly. At the beginning of the magnetic refrigeration system works, the HTF absorbs heat, which is generated by system's excitation. At the hot end of the system, the heat is released. The HTF gets a lower temperature and reaches the cold end for refrigeration. The T_h of the system increases with time, but the T_c decreases, according to the analysis.

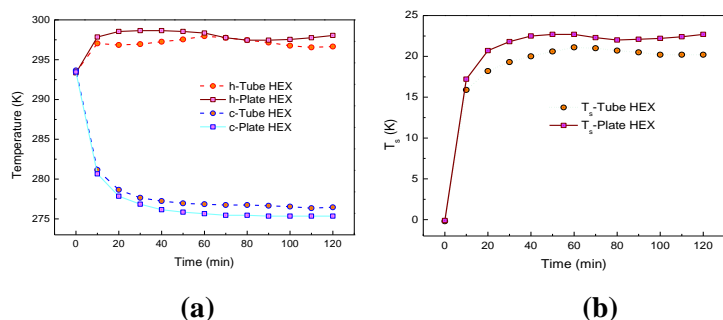


Fig. 11. Effect of structural changes of hot end heat exchanger

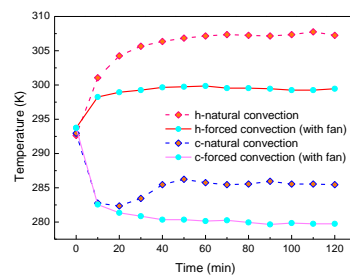


Fig. 12. The effect of heat dissipation method

3.3. Effect of AMR ports structure on the system performance

Figure 13 shows the variation of the system temperature at different kinds of active regenerators' port. It could be found that the temperature fluctuations that applying gradually varied port is more gentle than suddenly varied port when the T_c and T_h change gently. The T_c applying gradually varied port is less than the suddenly varied port. This mainly because that it's easier to produce the dead volume effect when applying the suddenly varied port, which leads to an uneven axial heat transfer of magnetic materials. But, the heat transfer of the fluid in the axial direction can be avoided when applying the gradually varied port. That is to say, heat exchanger fully with magnetic materials when the HTF passes through the gradually varied port of the AMR and the T_c decreases, so that the performance of the system is improved.

During the refrigeration cycle, the HTF releases heat at the hot end and reaches the cold end to refrigerate. The T_h of the system keeps increasing, and the T_c keeps decreasing, so the T_s between the cold and hot ends of the system will keep increasing. As shown in Fig. 13 (c), a maximum refrigeration T_s of 24.1 K can be achieved by the CMRS. The T_s applying gradually varied port is 1 K higher than suddenly varied port. Compared with the reciprocating magnetic refrigeration system [18] and the rotary magnetic refrigeration system [23], the comparison results show that the temperature span of CMRS has increased by 9% and 58%. Detailed parameters are shown in the Tab. 4.

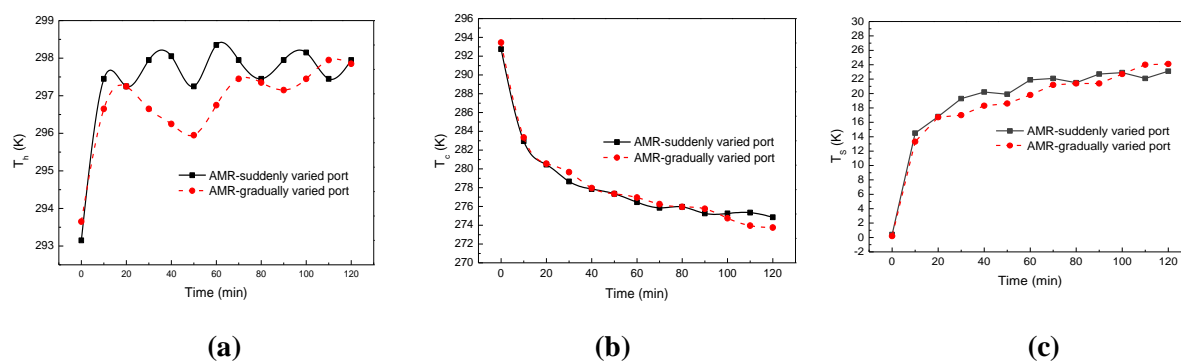


Fig. 13. Effect of aAMR ports structure on the system performance

Table 4. Equipment label of CMRS

| Type of the Magnetic Refrigeration System | Combined Magnetic Refrigeration System | Reciprocating Magnetic Refrigeration System [18] | Rotary Magnetic Refrigeration System [23] |
|---|--|--|---|
| Magnetic field source | Halbach permanent magnet blocks | Permanent magnets NdFeB | Permanent magnets NdFeB |
| Magnetic field | 0-1.3T | 1.45 T | 1.13 T-1.4 T |
| Magnetocaloric material | Gadolinium (Gd) | Gadolinium (Gd) | Gd and three different compositions of Gd _{100-x} Y _x |
| Mass of MCM | 1680 g | 800 g | 1700 g |
| Operation frequency | 0.2 Hz | 0.5 Hz | 0.75 Hz |
| Heat transfer fluid | A weakly alkaline deionized water | Silicon oil, zitrec, water | Demineralized water with 5% ethylene glycol based automotive antifreeze |
| Maximum temperature span | 24.1 K | 22.0 K | 10.2 K |

4. Conclusions

A combined magnetic refrigeration system (CMRS) using Gd as magnetic materials was designed, the performance of different structure for heat exchanger and active regenerator port was compared and analyzed based on this system. In this machine, a magnetic field varying from 0 to 1.3 T was provided by a double layer nested circular cylindrical concentric Halbach permanent magnets, and an weakly alkaline deionized water (PH=12) capable of inhibiting water ionization was used as the heat transfer fluid. During a certain range of operating parameters, a maximum 24.1 K temperature span of CMRS was obtained when using a gradually varied port of AMR.

Meanwhile, compared with a reciprocating magnetic refrigeration system [18] and rotary magnetic refrigeration system [23], CMRS has been increased by 9% and 58%, respectively. The T_s of HEX with inner surface threaded coil tube is 22.2 K, which is 0.8 K higher than that with smooth coil tube. A 22.7 K temperature span using plate HTX could be achieved, which is 2.5 K higher than the tube HEX. In addition, to improve the heat dissipation capacity of the system, the fan can be added to the HEX. Forced convection heat transfer can improve the refrigeration performance of the CMRS.

Acknowledgement

The authors are grateful to the financial support from National Natural Science Foundation of China (NSFC) (No. 51566014 and No. 51106068) and the Inner Mongolia Natural Science Foundation (No. 2021MS05035).

Nomenclature

| | |
|---------------------|--|
| B | magnetic field, T |
| L | length, m |
| T | temperature, K |
| V | volume, cm ³ |
| T _h | Hot end temperature, K |
| T _c | Cold end temperature, K |
| T _{cc} | Cold chamber temperature, K |
| T _s | temperature span, K |
| Abbreviation | |
| AMR | Active Magnetic Regenerator |
| CMRS | Combined Magnetic Refrigeration System |
| Gd | Gadolinium |
| HEX | Heat exchanger |
| HTF | Heat Transfer Fluid |
| MCE | Magnetocaloric effect |
| MCM | Magnetocaloric material |

References

- [1] Zheng, F. H., *et al.*, Numerical approach to solar ejector-compression refrigeration system, *Thermal Science*, 20 (2016), 3, pp. 949-952
- [2] Zheng, F. H., *et al.*, Solar ejector refrigerant system in China's residential buildings, *Thermal Science*, 18 (2014), 5, pp. 1643-1647
- [3] Wood, M. E., Potter, W. H., General analysis of magnetic refrigeration and its optimization using a new concept: maximization of refrigerant capacity, *Cryogenics*, 25 (1985), 12, pp. 667-683
- [4] Sarlah, A., *et al.*, Static and rotating active magnetic regenerators with porous heat exchangers for magnetic cooling, *International Journal of Refrigeration*, 29 (2006), 8, pp. 1332-1339
- [5] Russek, S. L., Zimm, C. B., Potential for cost effective magnetocaloric air conditioning systems, *International Journal of Refrigeration*, 29 (2006), 8, pp. 1366-1373
- [6] Lucia, U., *et al.*, General approach to obtain the magnetic refrigeration ideal coefficient of performance, *Physica A: Statistical Mechanics and its Applications*, 387 (2008), 14, pp. 3477-3479
- [7] Yao, G. H., *et al.*, Experimental study on the performance of a room temperature magnetic refrigerator using permanent magnets. *International Journal of Refrigeration*, 29 (2006), 8, pp. 1267-1273
- [8] Rowe, A., Configuration and performance analysis of magnetic refrigerators, *International Journal of Refrigeration*, 34 (2011), 1, pp. 168-177
- [9] Plaznik, U., *et al.*, Numerical and experimental analyses of different magnetic thermodynamic cycles with an active magnetic regenerator, *Applied Thermal Engineering*, 59 (2013), 1-2, pp. 52-59
- [10] Fortkamp, F. P., *et al.*, Analytical solution of concentric two-pole Halbach cylinders as a preliminary design tool for magnetic refrigeration systems, *Journal of Magnetism and Magnetic*

Materials, 444 (2017), pp. 87-97

- [11] Radel, G., *et al.*, Review on magnetic refrigeration devices based on HTSC materials, *International Journal of Refrigeration*, 100 (2019), pp. 1-12
- [12] Zimm, C., *et al.*, Design and performance of a permanent-magnet rotary refrigerator, *International Journal of Refrigeration*, 29 (2006), 8, pp. 1302-1306
- [13] Engelbrecht, K., *et al.*, Experimental results for a novel rotary active magnetic regenerator, *International Journal of Refrigeration*, 35 (2012), pp. 1498-1505
- [14] Luppunglung, V., *et al.*, Design and development of rotary magnetic refrigeration prototype with active magnetic regeneration system, Report No. 1380, Vancouver Convention Center, Vancouver, Canada, 2022
- [15] Huang, B., *et al.*, Development of an experimental rotary magnetic refrigerator prototype, *International Journal of Refrigeration*, 104 (2019), pp. 42-50
- [16] Zheng, H. Y., *et al.*, Design and performance study of the active magnetic refrigerator for room-temperature application, *International Journal of Refrigeration*, 32 (2009), 1, pp. 78-86
- [17] Arnold, D. S., *et al.*, Experimental analysis of a two-material active magnetic regenerator, *International Journal of Refrigeration*, 34 (2011), 1, pp. 178-191.
- [18] Balli, M., *et al.*, A pre-industrial magnetic cooling system for room temperature application, *Applied energy*, 98 (2012), pp. 556-561
- [19] Romero Gómez, J., *et al.*, A review of room temperature linear reciprocating magnetic refrigerators, *Renewable and Sustainable Energy Reviews*, 21 (2013), pp. 1-12
- [20] Velázquez, C., *et al.*, A comprehensive study of a versatile magnetic refrigeration demonstrator, *International Journal of Refrigeration*, 63 (2016), pp. 14-24
- [21] Romero Gómez, J., *et al.*, Magnetocaloric effect: A review of the thermodynamic cycles in magnetic refrigeration, *Renewable and Sustainable Energy Reviews*, 17 (2013), pp. 74-82
- [22] Tura, A., Rowe, A., Permanent magnet magnetic refrigerator design and experimental characterization, *International Journal of Refrigeration*, 34 (2011), 3, pp. 628-639
- [23] Eriksen, D., *et al.*, Design and experimental tests of a rotary active magnetic regenerator prototype, *International Journal of Refrigeration*, 58 (2015), pp. 14-21

Submitted: 22.01.2022.

Revised: 06.06.2022

Accepted: 09.06.2022.